Special Issue

Eletrônica de Potência
Open Journal of Power Electronics

Received July 30, 2026; Received in revised form October 16, 2026; Accepted October 27, 2026; Date of publication November 13, 2026.
The review of this paper was arranged by Associate Editor Montiê A. Vitorino and Editor-in-Chief Allan F. Cupertino.

Digital Object Identifier http://doi.org/10.18618/REP.e202641

Restructuring of an Undergraduate Course on Self-Commutated Converters and Power Quality

Lourenco Matakas Junior [1,*], **Vinicius N. Machado** [1], **Wilson Komatsu** [1], **Lucas Koleff** [1]

[1] University of São Paulo (USP), Polytechnic School, Electrical Energy and Automation Department, São Paulo, Brazil.

e-mail: matakas@usp.br*; vininegri.2000@gmail.com; wilsonk@usp.br; koleff.lucas@gmail.com
*Corresponding Author.

ABSTRACT This paper presents the restructuring of an undergraduate course of power electronics focused on self-commutated converters and power quality. It uses an active learning methodology that fully integrates experimental and theoretical classes. By intertwining theory and laboratory sessions without using practical classes merely to confirm the theory, the methodology enhanced learning and helped keep students motivated. In the authors' institution, student evaluation of the power electronics lectures is measured after the beginning of the course restructuring using statistical methods and has shown a steady increase in the number of students that are satisfied. Furthermore, the open-source platform and methodology can be freely used, adapted and extended, amplifying the impact across different universities and institutions.

KEYWORDS Education on Power Electronics, Power Electronics Experiments.

I. INTRODUCTION

The growth in the share of the consumed electricity, which is processed by power electronics equipment, boosted by the increased use of renewable energies, electric vehicles and smart grids, requires professionals with multidisciplinary knowledge, able to explain how they work, model, design and control them. It is difficult to be able to contextualize and motivate undergraduate students only with theoretical classes [1], [2], [3], [4], [5], [6], [7], [8], [9], [10], [11], [12], [13], [14], [15].

Java Applets are presented by [2]. Some authors focuses on proposing new experimental platforms and experiments [3], [5], [7], [8], [9], [12], [13], [14], [15]. To reduce development time and cost [9] proposes the efficient use of off-the-shelf hardware supplied by semiconductor companies.

Some papers, including this one, describe the use of different learning methodologies. Papers [10], [11], [13], propose Project Based Learning (PBL) strategies, where the students will have to model, design, construct and test a complete converter by themselves. Authors consider these methodologies the best approach to learn all aspects of a real-life converter, but it requires a reasonable workload allocated to the lecture, technical support (a reasonable number of lecturers, skilled technicians and graduate students) and laboratory infrastructure for the implementation and tests.

An intermediate step followed by this paper, similarly to [4], [6], [16], uses experimental platforms and strongly focuses on modelling, control, simulation, experiments and small projects. In [4], [6], [16], there is no discussion regarding learning outcomes or how the theory is taught, what is found in this paper.

The authors' experience in years of offering laboratory disciplines, one semester after the theoretical ones, was unsatisfactory. Several students do not remember or have not learned the theoretical concepts properly, limiting themselves to reproduce the experimental procedures, without understanding them. In addition, the authors did not have, until 2022, a complete experimental setup for Self-Commutated Converters (SCC), limiting themselves almost exclusively to the use of numerical simulation.

Over the past 10 years, an experimental platform, tailored for SCC learning, has been developed by the authors and their students [7], [8]. It allows: i) the experimental verification of the validity of the applied models for the considered hypotheses; ii) safe operation (30V, 1A), in line with Safety Extra Low Voltage (SELV) directives [17], [18], such as in [9]; iii) the use in undergraduate and graduate courses for rapid prototyping of small-scale models; and iv) disclosure as open-source hardware and software in the website [19], being open for other institutions, which can also contribute to the project, maximizing the global impact of the platform and methodology presented. This platform, shown in Fig. 1, has already been described in previous authors' papers [7], [8].

The development is not restricted to the course here presented but also valid for other institutions or groups facing similar issues, therefore, the authors are also sharing the resulting platform in an open repository [19]. Authors' papers about experimental platforms and learning methodologies are presented in [7], [8], [19], [20], [21].

The set of SCC experiments proposed is integrated in the Power Electronics courses offered by the authors' institution. The first offer was in 2022, focusing on a methodology that addresses the contents and develops the desired skills. The sequence of topics presentation during the SCC classes, based on Mohan [1], [16], uses the half-bridge converter as a basic cell, for the introduction of DC/AC - AC/DC and finally the DC/DC converters (uni/bidirectional and non-isolated/isolated ones).

The proposed restructuring focuses on active work during theory classes, interweaved with simulations and experiments

in laboratory classes. This includes: i) proposal of a new methodology, ii) development of an experimental platform, iii) proposal of the interweaving of theory and practical activities and iv) proposal of assessment strategies. This also creates an opportunity for authors and other lecturers to rethink and discuss the topic, exchanging experiences (in other forums) and provides a framework that can be readily applied in other institutions.

This paper is an extended version of the original version presented in [22].

The remainder of the paper is organized as follows: Section II briefly describes the methodology, Section III shows the designed and built experimental platform; Section IV presents the SCC course organization and discusses lectures contents and objectives; and finally, Section V the assessment of student performance, Section VI presents the students' evaluation of the course and Section VII the paper conclusions and future works.

II. PROPOSED LEARNING METHODOLOGY

In the last 40 years authors have been trying some learning strategies to improve their conventional theory and laboratory classes (separated one semester from the theory ones). For the theory classes they used:

i) Videos and texts for some flipped classes.

ii) List of exercises solving and small projects development in the theory classes, where the solution is available on the Moodle page of the course and on printed version. Students are said to try to solve the list, and to check the solution, step by step, alongside seeing colleagues' solution, and discussing with them. At first, students consider it is a joke, but in a few minutes, they are enthusiastically discussing their solutions and helping each other. Lecturers walk around the room, to contribute to help students, especially regarding questions related to knowledge gaps in previous subjects. It is a good chance to review and clarify then. Students with new solutions are invited to present them on the whiteboard for the colleagues. Students are encouraged to trust their solution and defend it. If they are wrong, the lecturer or their peers take it upon themselves to point out the error.

iii) Seminars, where each group prepares and presents some specific topic not treated along the classes. They are encouraged to present products developed and constructed by themselves and show demonstrative experiments.

iv) Design, followed by implementation, discussion of tests procedures, and demonstrative tests in the theory classroom. This strategy was used for classes regarding inductor and transformer design, where the component is designed, implemented and tested in the classroom. It is a fast and effective way to discuss implementation issues when related laboratory classes are not available. For the laboratory classes, they used:

- Pre-prepared demonstrative experiments;
- Presentation of components (power semiconductors, various heat sinks, transducers, etc.) and high-power converters available in the laboratory to demonstrate implementation details.
- Walkthrough of the building to take power quality measurements, etc.
- Extra activities for interested students to carry out outside of class hours.

The restructuring of the power electronics courses considered the following restrictions:

i) The former two semestral theory classes (four hours/week) and two laboratory classes (two hours/week), half of them dedicated to line commutated and half of them to self-commutated converters. The new self-commutated course should include theory and laboratory in four hours/week.

ii) In the 8th semester, students have to attend a total of 390 hours of lectures, and many are engaged in academic internship. They have limited time available for activities outside the classroom;

iii) The aging and retirement of the program's faculty, combined with insufficient replacement, mean that the program currently cannot support teaching strategies requiring a large number of instructors.

iv) The curriculum requires students to have a comprehensive view of Power Electronics, with a strong focus on modeling, simulation, experimentation, and grid applications.

According to the Introduction section, regarding the PBL methodologies:

i) Authors consider them the best approach for learning [10], [11], [13].

ii) PBL requires a large number of students hours outside classroom [10], [11], [13]. If the student's workload is not officially allocated in the curriculum and other courses decide to use PBL, students will face problems.

iii) it requires skilled technicians and graduate students, and a reasonable number of lecturers.

iv) PBL does not accommodate a comprehensive presentation of power electronics. References [4], [6], [16] do not provide details, but it is understood that a broad overview is provided through conventional lectures. However, a few projects allow for an in-depth understanding of the processes of modeling, control, design, implementation, and testing.

Considering the above listed restrictions, and considerations about PBL, this methodology was not viable when this course was planned.

On the other hand, [4], [6], [16] rely heavily on modeling, simulation, projects, and experiments, fitting well within a conventional curriculum. They do not address how theoretical classes are conducted or how assessment is carried out. Combining this proposal with the authors' experiences in employing more efficient teaching and learning strategies resulted in the methodology proposed below. Its main points are:

i) To carefully integrate theoretical and laboratory lessons, with theory also introduced during laboratory activities, so practical classes confirm theoretical aspects, reveal learning needs and motivate students for subsequent theoretical classes;

ii) To focus on the modeling process and verification of its validity, via simulation and experiments;

iii) To concentrate on instrumentation, experiment planning, data post-processing, and details that include verification of the sampling rate effect, A/D converter resolution, noise, offset of current and voltage channels on post-processed results and mitigation of these problems;

iv) Power quality aspects are treated along the course;

v) Instead of passively taking notes on the lecturer's presentation, students are guided during theory classes to actively draw the converter waveforms, and develop the equations by themselves.

As a result of the application of the proposed methodology, students are able to develop their abilities and excel in: a) modelling the phenomenon using simplifying hypotheses; b) validating models through simulation and experiment; c) verifying model inadequacies when hypotheses are not met; d) proposing improvements in the model, verifying that they inevitably lead to more complex models that require more parameters, which must be calculated theoretically or determined experimentally. This strategy can be used in other engineering disciplines involving modeling. The authors have already successfully used it for other subjects [20], [21], and recently to Line Commutated Converters classes (not yet disclosed in papers).

A comprehensive review and comparison to other learning methodologies is out of the scope of this paper.

III. EXPERIMENTAL PLATFORM FOR LEARNING SELF-COMMUTATED CONVERTERS, AND THEIR ASSOCIATED POWER QUALITY ISSUES

The developed platform (Fig. 1) has a philosophy similar to that of other power electronics training kits [1], [3], [4], [5], [6], [9], [12]. Additionally, it operates with low voltage (30V) and current (1A), ensuring compliance with SELV [17], [18], reducing the risk of injury to the user and the risk of damage to equipment. Low power leads to a low-cost platform, which is a positive aspect compared to commercial options. It is available as open-source hardware and software [19], so that it can be used by other Educational Institutions and interested parties, which is also an advantage to closed-source options. Each of the full Platforms (Fig. 1) contains:

A) One 3-phase 4-wire converter: consisting of two low-cost H-bridge Ics (LM6203), whose gate signals are optically isolated with HCPL-2200 optocouplers;

B) One 32 bits ARM microcontroller-based processing board (using the low-cost development board STM32F4DISCOVERY). This board is connected to the converter board, the power supply, and the voltage and current transducer boards via flat cables that carry signals and power supply buses;

C1) 3-phase adjustable resistive loads (wye connection – each phase with 6 resistors of 100Ω/10W connected in parallel via switches);

C2) Single-phase adjustable resistive load (6 branches of 150+150Ω/10W connected in parallel by means of switches);

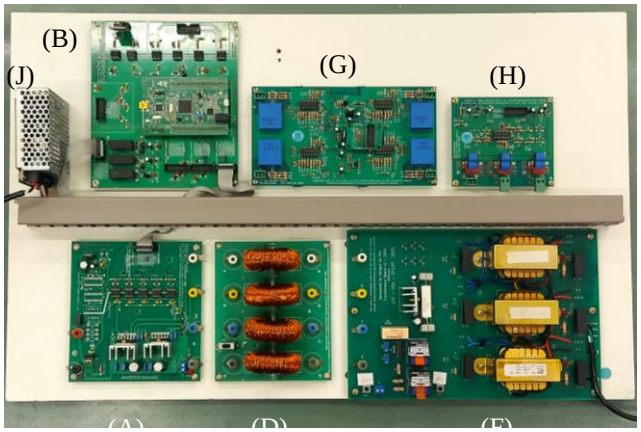
D) Two inductive filter boards, each one with four series inductors (3.5mH @ 1A, Q=5 @ 60Hz), one for each phase including the neutral terminal. This last one can be short circuited by a switch. They employ iron powder toroidal cores for reduced losses and nearly linear magnetic behavior. They allow the implementation of filters with L (3.5 mH), L+L (7 mH), LC, (L+L)C and LCL;

E) Capacitive filter board: it has two 4.7μF film capacitors connected between each phase (A,B,C) and the neutral terminal (N). For each pair of capacitors, one of them has a series 39 Ω that can be short circuited by a switch. It provides the possibility to explore the undamped behavior of the LCL filter, and its passive damping in undergraduate courses. For higher-level courses, active damping strategies can be explored;

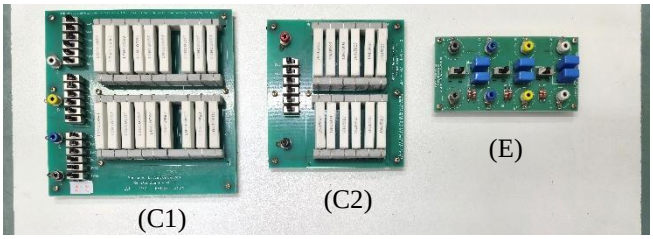
F) One 3-phase delta-wye (line RMS $220 - 12\sqrt{3}$ V) transformer board for experiments connected to the grid. It contains three low cost 220/12V (RMS) – 36VA single-phase transformers. Usually, experiments will use peak currents lower than 0.5A (peak). The reason for using an oversized component, for $3\sqrt{2}$A (peak), is to be able to do experiments in nearly idealized strong grid conditions. For weak grid experiments the inductor board can be added. It has one 3-phase relay for switching on and off the board output, and a second one, for automatically inserting pre charging series resistors when inverters are connected to the grid. This second relay is commanded by comparators and logic implemented by reed relays, to include the series resistors when the inverter DC bus voltage is low and short circuit then as soon as this voltage reaches the predefined value, adjusted by potentiometers. Overcurrent protection is done by fuses at the primary and secondary sides;

G) Voltage transducers board: it has 4 measuring channels (-40V~+40V input / 0~3V output), each one implemented with a Hall effect transducer (LEM LV25-P) and three cascade operational amplifiers for signal conditioning (level and offset adjust and low pass filtering). It can be used for example to measure 3 AC voltages in 4-wire systems and one DC voltage;

H) Current transducers board: it has 3 measuring channels (-1.6A~+1.6V input / 0~3V output), each one implemented with a Hall effect transducer (LEM LTS 6NP,) and operational amplifiers for signal conditioning (level and low pass filtering);



(a)



(b)

FIGURE 1. Parts used in the platform a) left to right – Top: (J), (B), (G) and (H); Bottom: (A), (D) and (F); b) left to right: (C1), (C2) and (E).

I) A PC based human machine interface (HMI) to operate the platform. The program, that contains all experiments used during the course, is previously loaded in the microcontroller.

Students use the HMI to choose the desired experiment and related parameters. It is important in a short class (100 minutes), to avoid students' errors during program changes and reloading, that could damage the boards;

J) DC power supply (±15 & 5V): it powers the processing board directly. The converter and transducers boards are fed by their respective flat cables together with the command and measured signals.

IV. ORGANIZATION OF THE COURSE ON SCCs AND A BRIEF DISCUSSION FOR EACH TOPIC

Power Electronics undergraduate classes at the authors' institution are divided into two courses (1 semester each), one for Line Commutated Converters (LCC), and the second for Self-Commutated Converters (SCC). This does not limit however the application in other institutions. Introductory Power Quality (PQ) was presented in the first lecture of the previous LCC course, where PQ issues (current harmonics, voltage harmonics, power factor, displacement factor, total harmonic distortion (THD), etc.) are discussed for each converter. The topics of PQ are presented briefly here because they have already been discussed in more detail by the authors in [21]. Greater focus will be given to classes involving SCC, including the study of the half-bridge converter, considered as a basic cell for the analysis, modelling and control of the H-Bridge, the 3-phase and the DC/DC converters. Together with the experimental platform described in Section II, PSIM is used for circuit simulation, and MATLAB is used to post process measured voltage and current waveforms to obtain the active power, THD, displacement factor, spectra, among other calculations.

In each theoretical class, students are guided to understand the operation of the new converter topology, obtaining the basic relationships between voltages and currents that allow them to draw the main waveforms, calculate the relevant variables (active power, average and RMS values, power factor, ripple, harmonics, etc.) and, finally, create design recipes when possible. The student constructs their own knowledge, not just by attending and taking notes in class. It is an excellent opportunity for the student to identify learning deficiencies and address them with classmates or the lecturer, during the class.

The undergraduate course on SCC totalizes around 30 classes (100 minutes each one). This session uses the following abbreviations: a) Theory classes - T, b) Laboratory classes - L, c) Experiments - E, and d) Simulation - S. It covers the following topics:

A. *PQ I: VOLTAGE DISTORTION AT THE POINT OF COMMON COUPLING (PCC) AND HARMONIC CURRENTS IN POWER FACTOR CORRECTION CAPACITORS (1T+1L(E)) [21]*

In the first theory class of the Self Commutated Converters Course, a single-phase inductive grid is modelled by its equivalent Thevenin circuit, and feeds a non-linear load modelled as a set of paralleled current sources, one for each harmonic component. Students obtain the equations for the spectra of the (PCC) voltage, and numerically calculate them for a set of parameters previously chosen by the lecturer. A capacitor is inserted in parallel with the load at the PCC, and students obtain the equations for the capacitor current spectra and the new PCC voltage spectra, showing that this last one depends on the capacitor. Numerical values are calculated for the parameters chosen to present a resonant frequency near 225Hz (3.76 x 60Hz). Parallel resonance and the resulting voltage amplification, together with the increase of the amplitude of the fundamental PCC voltage are discussed.

The laboratory class uses a 12V nonlinear load consisting of an 80~250V, 3W, low power factor, bulb type LED lamp fed by a 12/220V, 6VA transformer. In addition to its very low cost and ease of implementation, this load exhibits rich harmonic content due to the rectifier with capacitive filter of the lamp, added to the lagging and distorted current due to the magnetizing current of the transformer. This load is fed by the transformer board.

At first the load is connected to the strong grid and then to a weak grid (emulated by the inclusion of a 3.5mH inductor). Students verify that:

- The load current spectrum is affected by the grid impedance, contrary to the assumption of an invariant spectrum made in the theoretical class, but it still provides reasonable results;
- The experimental spectrum of the PCC voltage is consistent with that deduced in the theory class;
- The inclusion of a 20μF capacitor in parallel with the load, validates the theoretically calculated current spectra in the capacitor and voltage spectra across the PCC;
- When the capacitor is connected alone to the electrical grid, its current exhibits a fairly broad spectrum, as its reactance decreases with frequency, offering a low-impedance path for higher-order harmonic currents present in the grid.

B. *PQ II: PASSIVE COMPENSATION OF LOAD UNBALANCE (1T+1L(S))*

The Steinmetz [23] inspired circuit for compensating load unbalance for a single phase, linear inductive load connected between phases A and B, modelled as a parallel connection of one inductor with impedance jX_1 and a resistance R_1 (Fig. 2a), is presented in Fig. 2b. The combined reactive power and unbalance compensator (Fig. 2b) includes three components: a) a capacitor with impedance $-jX_1$ to fully compensate load power factor; b) a capacitor between phases B and C, and an inductor between C and A, with impedances $-j\sqrt{3}R_1$ and $+j\sqrt{3}R_1$ respectively.

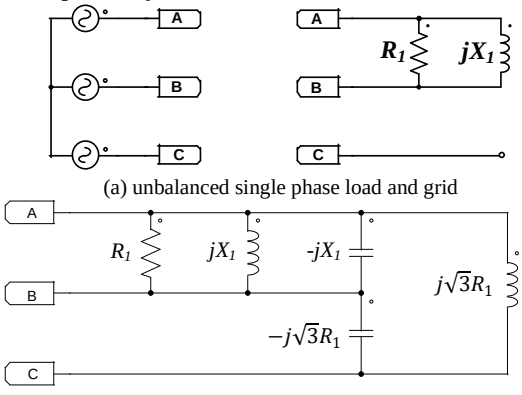


FIGURE 2: Unbalance compensator

In the theory class students:

- Calculate the three line currents and verify that they have the same amplitude and are in phase with their respective phase voltages;
- Calculate the symmetrical components for the currents in the load, compensator and line and show that the compensator has a pure balanced capacitive positive sequence current that compensates the load reactive power and a negative sequence component, that compensates the load negative sequence current. This results in positive sequence line currents, in phase with the voltages positive sequence;
- For the generic delta connected load in Fig. 3, composed by $R_1//jX_1$, $R_2//jX_2$ and $R_3//jX_3$, they use the result for single phase load and the superposition theorem to obtain the impedances of the delta connected unbalance compensator (Z_{AB}, Z_{BC}, Z_{CA}), shown in Fig. 3.
- Verify that the resulting compensator impedances (Z_{AB}, Z_{BC}, Z_{CA}). are inductors or capacitors, with null active power. The lecturer emphasizes that SCC can inject arbitrary currents and can be used to emulate the behavior of compensator impedances (Z_{AB}, Z_{BC}, Z_{CA}).

In the laboratory class students:

- Numerically calculate, using MATLAB, for a given generic load composed by $R_1//jX_1$, $R_2//jX_2$ and $R_3//jX_3$:
  - the compensator impedances Z_{AB}, Z_{BC}, Z_{CA};
  - the phase currents for the load, compensator and line, and their symmetrical components;
  - the active and reactive power for each phase, for the load, compensator and line (obtained by using the grid voltages, represented by the phasors $\dot{V}_a$, $\dot{V}_b$, $\dot{V}_c$, and the line currents for the load $\dot{I}_a$, $\dot{I}_b$, $\dot{I}_c$, compensator $\dot{I}_{comp_a}$, $\dot{I}_{comp_b}$, $\dot{I}_{comp_c}$ and grid $\dot{I}_{line_a}$, $\dot{I}_{line_b}$, $\dot{I}_{line_c}$).

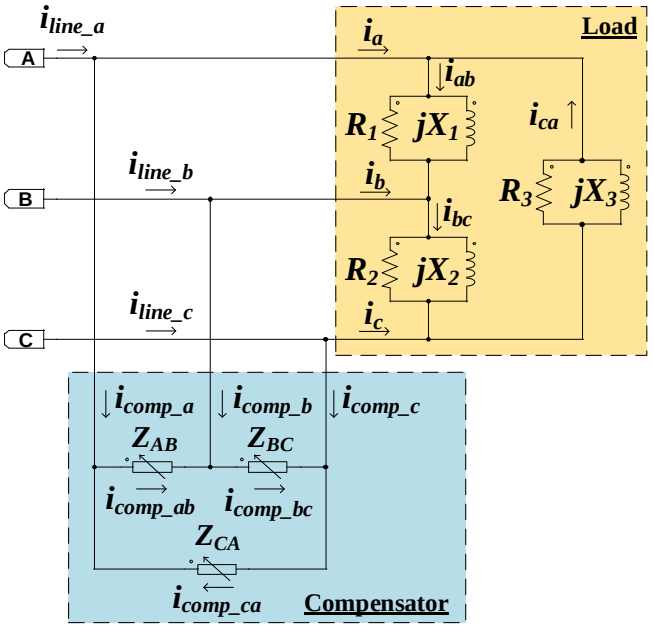


FIGURE 3. Upper block: generic load; Lower Block: Generic delta connected unbalance compensator

- Verify the effectiveness of the compensation strategy by the analysis of the line currents, per phase active and reactive power and by the symmetrical components;
- Verify that the active power per phase in the compensator is not zero, contributing to the redistribution of the active power of the unbalanced load. However, the sum of the powers per phase is zero;
- Validate the calculated values by circuit simulation;
- Verify by simulation that this compensator is highly sensitive to changes in the load and to the inversion of the phase sequence of the grid voltages;
- Simulate the energization of the previous load plus the compensator circuit when fed by a transformer, showing decaying high frequency transients caused by the excitation of the circuit poles;
- Understand the lecturer presentation of a real case occurrence of series resonance in a 4.5MVA industry after the inclusion of Steinmetz compensator, that caused severe overcurrents, opening the circuit breakers [24]. A passive solution consisting of the inclusion of inductor for resonance detuning is discussed.

C. *PASSIVE FILTER (1T+1L(S))*

In the theory class, the operation principle of conventional parallel association of series connected LC filters [25], [26] is analyzed. Students:

- Calculate the attenuation for h^{th} order harmonic current, verifying its dependence on the grid impedance and the resistance of the filter inductor;
- Verify that each LC branch has capacitive behavior at fundamental frequency, and this can be considered for compensating the load displacement factor (if inductive);
- Develop an initial strategy for designing one branch of the LC filter.

In the laboratory class, students:

- Validate for one filter branch, by simulation, the simplified design method developed at the theory class;
- Verify by simulation that the passive filter is not selective, absorbing harmonics from neighbor loads;
- Include a second filter branch and verify that the increase of capacitive current and the branches interdependence must be considered for a real filter design [25].

D. *CURRENT HARMONICS IN 3-PHASE SYSTEMS (1 L(E)) [21]*

For wye (4-wire) and delta connected LED bulb lamps (15W, 85~250V, PF=0.7) students:

- Measure line and neutral currents for balanced and unbalanced 3-phase nonlinear loads (for the wye case);
- Measure line and phase currents for balanced and unbalanced 3-phase nonlinear loads (for the delta case);
- Verify that for wye balanced load: a) the 1st, 7th, 13th, 6k+1, k=0,1,2,3… line current harmonics have positive sequence behavior; b) the 5th, 11th, 6k-1, k=1,2,3,… etc. are of negative sequence; c) the multiples of 3 are zero sequence components that flow through the line and neutral conductors; and d) the fundamental frequency of the neutral current is three times the grid frequency;
- Verify that for delta balanced load: a) the 1st, 7th, 13th, etc. phase current harmonics have positive sequence behavior; b) the 5th, 11th, etc. are negative sequence; c) the multiples of 3 are zero sequence components that flow inside the delta, and are not present in line currents;
- Verify that for wye and delta unbalanced load, each harmonic of the phase currents has components of the 3 sequences. In a wye connection, the current in the neutral conductor contains only zero-sequence components,

CC BY

exhibiting all frequencies of the phase current spectrum. In the delta connection, zero sequence components will not appear in the line currents. This important fact is unknown to many students and professionals, who believe that the results for balanced loads extend to unbalanced loads. This is a good opportunity to understand it.

E. *HALF BRIDGE VOLTAGE SOURCE CONVERTER (VSC) (2T+2L(1S+1E)*

The half-bridge converter (Fig. 4) will be considered as a basic cell for the next studied topologies. Natural sampled PWM (Fig. 4) is used in this course. Regarding the MATLAB functions used to post process the measured waveforms, for this particular class, details like noise, offset and also the aliasing effect on the calculated signals spectra, etc. are discussed.

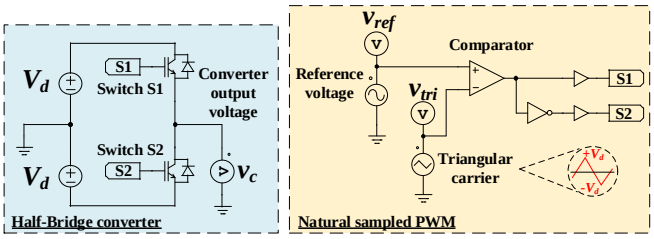


FIGURE 4. Half Bridge converter with natural sampled PWM

In the first theory class students:

- Check that the output voltage v_c is a two-level signal ($-V_d$; $+V_d$) that can be pulse width modulated (PWM) so as to make its local average $\hat{v}_c$ vary from $-V_d$ to $+V_d$.
- Prove that the simple natural sampled PWM [27] strategy, shown in Fig. 4, assures that $\hat{v}_c$ is locally equal to the PWM block reference signal v_{ref};
- Learn, without rigorous mathematical proof [27], [28], that for sinusoidal v_{ref}, the output voltage v_c presents a well-behaved spectrum, where the fundamental component is equal to the v_{ref} amplitude. The remaining harmonics are concentrated in groups around the multiples of the carrier frequency, that is equal to the switching frequency f_s [27], [28];
- Calculate the current spectrum for a resistive load R with series L filter;
- Calculate the inductor current and output voltage spectrum for a resistive load R with LC filter;

In the second Theory class students:

- Carry out time domain analysis to obtain the equations to calculate the peak to peak current ripple at inductor;
- Verify that this equation is also valid approximation for current ripple calculation in LC and LCL filters;
- Verify that the maximum current ripple occurs for $v_{ref}=0$.

Students confirm all the topics of the two previous theory classes by simulation in idealized conditions in the first laboratory class and by experiments in the second laboratory. Due to the difficulty of balancing the DC side capacitors in a half-bridge converter, experiments are carried out with an H-Bridge converter with bipolar PWM (2 levels). Initial operation is carried out using v_c with 30V peak value, R=20Ω, L=3.5mH, f_s=1.2kHz.

Important topics that require students' attention are:

- The occurrence of PWM saturation, for $|v_{ref}|>V_d$, results in a fundamental component of v_c that is smaller than the amplitude of v_{ref}. Low-frequency harmonics, which are difficult to filter out, also appear. Students learn that saturation must be avoided for the correct operation of the converter together with its control loops. For $|v_{ref}|\leq V_d$, the local average is $\hat{v}_c=v_{ref}$, and the first high frequency harmonics appear only at the neighborhood of f_s. For this experiment, a 300 Ω resistor (without L) is used to ensure not only minimal current for the correct turn-on and turn-off of the switches, but also low voltage drops at the switches, obtaining nearly idealized waveforms and respective spectra;
- For 2-level signals the amplitude of the high frequency undesired harmonics increases for operation with decreasing amplitudes of v_{ref};
- Discussion of the convenience and consequences of increasing the filter inductance L or the switching frequency f_s for reducing the current ripple, after doing experiments and simulations separately increasing L (7 to 14mH) and f_s (1.2 to 2.4 kHz);
- Discussion of the effect of the voltage drops on the MOSFET transistors ($R_{DS_ON}=0.3\ \Omega$) and antiparallel diodes, affecting the idealized squared wave v_c and its spectra, especially the fundamental component. Fig. 5 presents the waveforms of current dependent output voltage v_c and load current i for R=20Ω, L=7.0mH, f_s=1.2kHz, and DC H-Bridge voltage source of +30V.

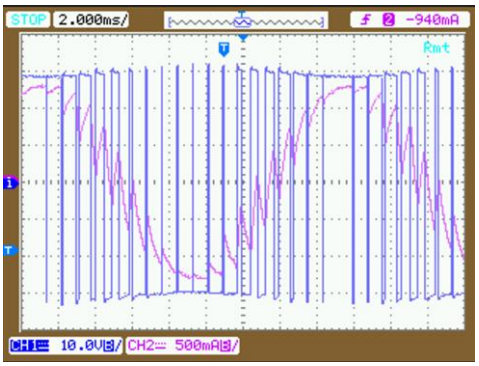


FIGURE 5 - v_c and i for the H-Bridge converter – effect of transistor/anti-parallel diode voltage drop (experimental results).

F. *H-BRIDGE CONVERTER (1L(T+S+E))*

This laboratory class mixes theory, simulation and experiment. The H-Bridge converter (Figs. 6 and 7) is analyzed as consisting of two half-bridges (basic cell) with output voltages v_{AX}, v_{BX}. So, its output voltage is $v_{C_AB}=v_{AX}-v_{BX}$. The half-bridge dual voltage source (V_d+V_d) and the central point X is shown only for analysis purposes, but students are lectured that real applications use the single voltage source $V_{cc}=2V_d$.

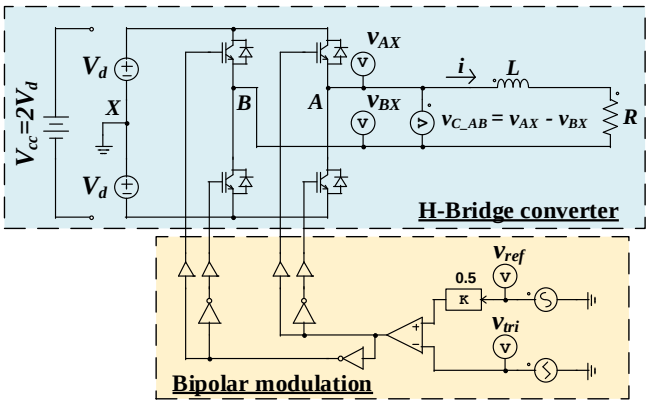


FIGURE 6 - H-Bridge converter formed by two half-bridges - bipolar modulation

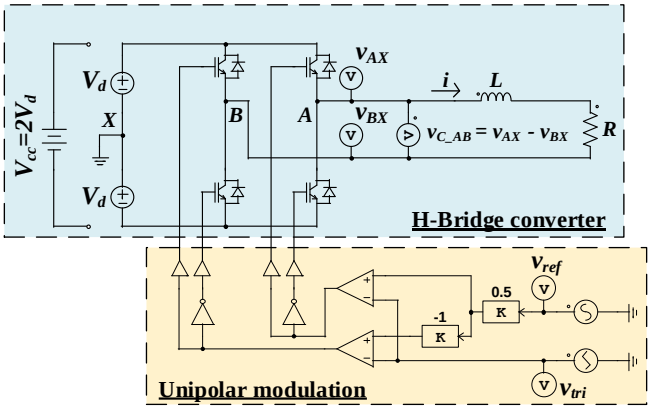


FIGURE 7 - H-Bridge converter formed by two half-bridges - unipolar modulation.

Students' tasks are to:

- Verify the H-Bridge has naturally a 3-level converter at v_{C_AB}. Additionally, the H-Bridge can operate either with two levels by using the bipolar PWM (Fig. 6) or with three levels with the unipolar PWM (Fig. 7). The second one produces less distorted current waveforms, but higher common mode high frequency voltages that can be undesirable when considering PQ and EMI issues;
- Verify that, for the same specified output voltage and current, when compared to the half-bridge, despite using four switches, the H-Bridge requires DC source V_{DC} and switches voltage ratings half of the values required for the half-bridge case;
- Use a template to draw, by hand, v_{AX}, v_{BX} *and* v_{C_AB} for bipolar and unipolar PWM, showing that for the second one, in addition to the three voltage levels, the number of transitions per switching cycle doubles;
- Calculate the current ripple for L filter in time domain, for three level v_{C_AB} , showing that the joint effect of increasing the quantization levels and equivalent frequency, results peak to peak current ripple four times lower than the ones presented by the bipolar modulation;
- Learn that the H-Bridge can be considered as a simple form of cascaded converter because $v_{C_AB}=[v_{AX}+(-v_{BX})]$, and this principle of harmonics cancelation can be extended to arbitrary connection of series converters [29];
- Validate the theory by simulations and experiment, additionally showing that the voltage has three levels, reducing the current ripple by a factor of four, and that the spectra of the output voltage and current only shows high frequency harmonics in the neighborhood of $k2f_s$ *(k=1,2,3,…).*

G. *OPEN LOOP OPERATION OF 3-PHASE 3-WIRE CONVERTER (2T+1L(S+E)*

In the 1st theory class, 3-phase converter is presented as three half bridges sharing the same dual power supply (Fig. 8a), that can be modelled as three two level Wye connected voltage sources $[v_{ca}, v_{cb}, v_{cc}]=[v_{aG1}, v_{bG1}, v_{cG1}]$, with common node G1, according to Fig. 8b. Fig. 8c presents the decomposition of $[v_{ca}, v_{cb}, v_{cc}]$ in a zero-sequence voltage v_{cz} and a set of voltages $[\bar{v}_{ca}, \bar{v}_{cb}, \bar{v}_{cc}]$, where: $\bar{v}_{cx}=v_{cx}-v_{cz}$, $x=a,b,c$. Natural sampled PWM with the same triangular carrier is used. During the class, students:

- Verify that the load voltages $[v_a, v_b, v_c]$ are equal to $[\bar{v}_{ca}, \bar{v}_{cb}, \bar{v}_{cc}]$;
- Draw by hand, in a template, the waveforms of $[v_{ca}, v_{cb}, v_{cc}]$, v_{cz}, $[\bar{v}_{ca}, \bar{v}_{cb}, \bar{v}_{cc}] = [v_a, v_b, v_c]$ and the current ripple for i_a. They conclude that the set $[\bar{v}_{ca}, \bar{v}_{cb}, \bar{v}_{cc}]$ has no zero-sequence component, as it is contained in v_{cz}. They also calculate the local average of $[v_{ca}, v_{cb}, v_{cc}]$ and $[\bar{v}_{ca}, \bar{v}_{cb}, \bar{v}_{cc}]$ to check that they are equal to the corresponding PWM reference signals $[v_{ca_ref}, v_{cb_ref}, v_{cc_ref}]$. Improvement of the THD of the output signals for the 3-phase case, compared to the single phase one is discussed.
- Verify that $[v_a, v_b, v_c] = [\bar{v}_{ca}, \bar{v}_{cb}, \bar{v}_{cc}]$ are 5-level signals;

In the 2nd theory class, students:

- Prove that the injection of a zero-sequence signal v_{cz_ref} to the PWM references $[v_{ca_ref}, v_{cb_ref}, v_{cc_ref}]$ cause no change in the local average of the load voltages $[v_a, v_b, v_c]$, by hand-drawing all the waveforms, similar to the 1st class. The shape of the load current, excluding its high frequency harmonics, is not affected by v_{cz_ref}, because this component cannot inject currents in a 3-phase, 3-wire system.
- As the 3-phase converter is modeled as three half-bridges, students conclude that the maximum voltage that can be synthesized in each phase is V_d. Consequently, the maximum phase to phase synthesizable amplitude is $\sqrt{3}V_d$. The lecturer points out that the voltage between two phases is identical to the voltage produced by a H-bridge, whose maximum output voltage is $2V_d$, 15% higher than $\sqrt{3}V_d$, with the same DC voltage. This limitation, imposed by the individual natural sampled PWMs can be overcome by injecting a specific chosen instantaneous zero-sequence signal (v_{z_opt}) to the three original references, defined by (1), or by using a Space Vector Based PWM [30], [31] (not discussed during the class).

$$v_{z_opt}=0.5[\max(v_{cx_{ref}})+\min(v_{cx_{ref}})] \text{ for } x=a,b,c \quad (1)$$

- Using a template, draw by hand the ripple at the load current and conclude that it is affected by v_{cz_ref}, and is minimized for $v_{cz_ref}=v_{z_opt}$

In the laboratory class, Students validate the theory by using numerical simulation (PSIM) and experiments. According to Fig. 8a, $V_d=V_{dc}/2$, where V_{dc} is the converter DC voltage. For the experiments and simulation: $V_{dc}=30V$, switching frequency f_s =2.4 kHz, L=3.5mH (when the inductive filter is required), R=16.6Ω (when the resistive load is required). The first activity of this laboratory lecture is to show the operation with 60Hz, positive sequence reference signals, with peak value of 15V=$V_{cc}/2$. No zero sequence is added to the references.

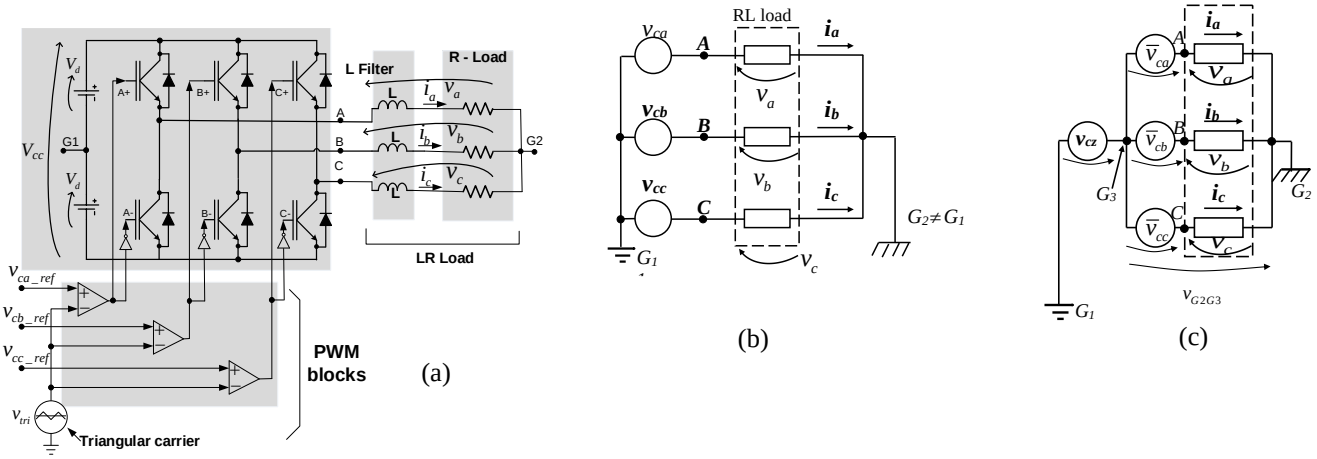


FIGURE 8 a) 3-phase converter, b) equivalent model, c) decomposition in v_{cz} and $[\bar{v}_{ca}, \bar{v}_{cb}, \bar{v}_{cc}]$.

To avoid the use of three current probes, the voltages at the three load resistors are measured, according to Fig. 9. Although these signals are only acquired and not post-processed, Fig. 9 is very useful for quick estimates, so that students:

- Verify that the resistors' voltages (proportional to the currents) are nearly sinusoidal, balanced positive sequence signals, with fundamental peak amplitude slightly lower than the expected value of 15V, due to the MOSFET resistance, anti-parallel diode, and inductor voltage drops;
- Estimate the switching frequency;
- Validate results by simulation.

Next, students:

- Verify that operating with modulation index (m) out of the region ±100% ($m=100\%\cdot v_{ref}/V_d$), with $v_{cz_ref}=0$, causes saturation of the PWM. This is the limit of the individual half bridge converter.
- Verify and are asked to explain that the injection of $v_{cz_ref}=v_{z_opt}$ (1) enables the operation with m as high as 115% without saturation, shown in the simulation of Fig.10, which includes: a) the three PWM reference signals [$v_{ca_{ref}}$, $v_{cb_{ref}}$, $v_{cc_{ref}}$], with amplitude 1,15V (for $V_d=1V$) ; b) the zero sequence injected signal $v_{cz_ref}=v_{z_opt}$; and c) the new reference signal for phase A [$v_{ca_{ref}}+v_{z_{ref}}$]. The addition of $v_{cz_ref}=v_{z_opt}$ flattens the top of the original reference signals, making them lower than V_d , avoiding PWM saturation. Additionally, $v_{cz_ref}=v_{z_opt}$ does not contribute to the AC currents in a 3-phase 3-wire circuit.

Fig. 11a and b presents the 2-level voltage v_{ca} , at the output of the phase A half-bridge, and its spectrum. Fig. 11c and d presents the 5-level LR load voltage ($v_a=\bar{v}_{ca}$) and its spectrum. Fig. 11e and f present the current at phase A and its spectrum.

Next, the spectra of v_{ca} , $\bar{v}_{ca}$ and i_a are analyzed and discussed, concluding that the spectra of $[\bar{v}_{ca}, \bar{v}_{cb}, \bar{v}_{cc}]$ contain neither the third harmonic corresponding to v_{z_opt} nor the high frequency zero-sequence components [30], [31], [32], both present at $[v_{ca}, v_{cb}, v_{cc}]$. As a consequence, $[i_a, i_b, i_c]$ also do not present them and have a lower THD, compared to the 2-level half bridge converter or to the 3-phase / 4-wire converter obtained by connecting G1 and G2 together. The current harmonics are calculated for the fundamental frequency and for a frequency neighboring f_s, and compared to simulated and experimental ones.

It is important to emphasize the effect of voltage drop at the converter MOSFET switches, and anti-parallel diodes, clearly seen at v_{ca} in Fig. 11a, and that it can be easily considered in the simulation by including R_{DS_ON} resistance and diode voltage drop.

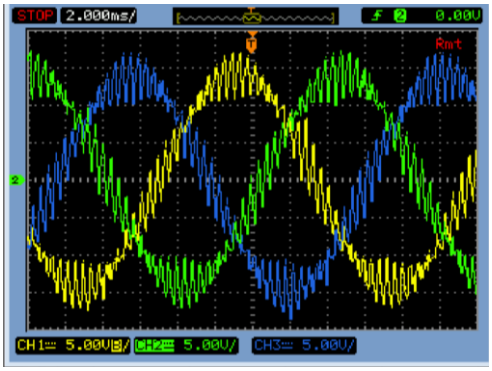


FIGURE 9. Voltages at the three wye connected resistive load: phases a,b,c (*m=100%*) are respectively yellow, green and blue (experimental results).

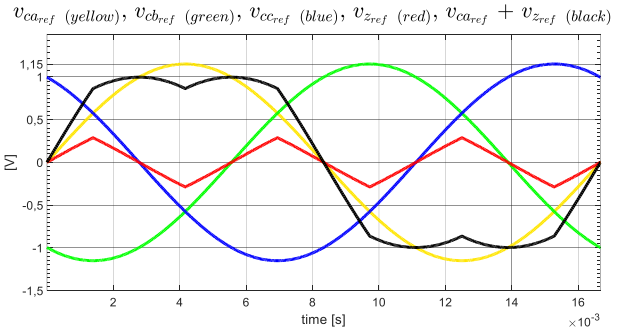


FIGURE 10. Waveforms of $v_{ca_{ref}}$, $v_{cb_{ref}}$, $v_{cc_{ref}}$, v_{z_ref} and $v_{ca_{ref}}+v_{z_{ref}}$ (simulation results).

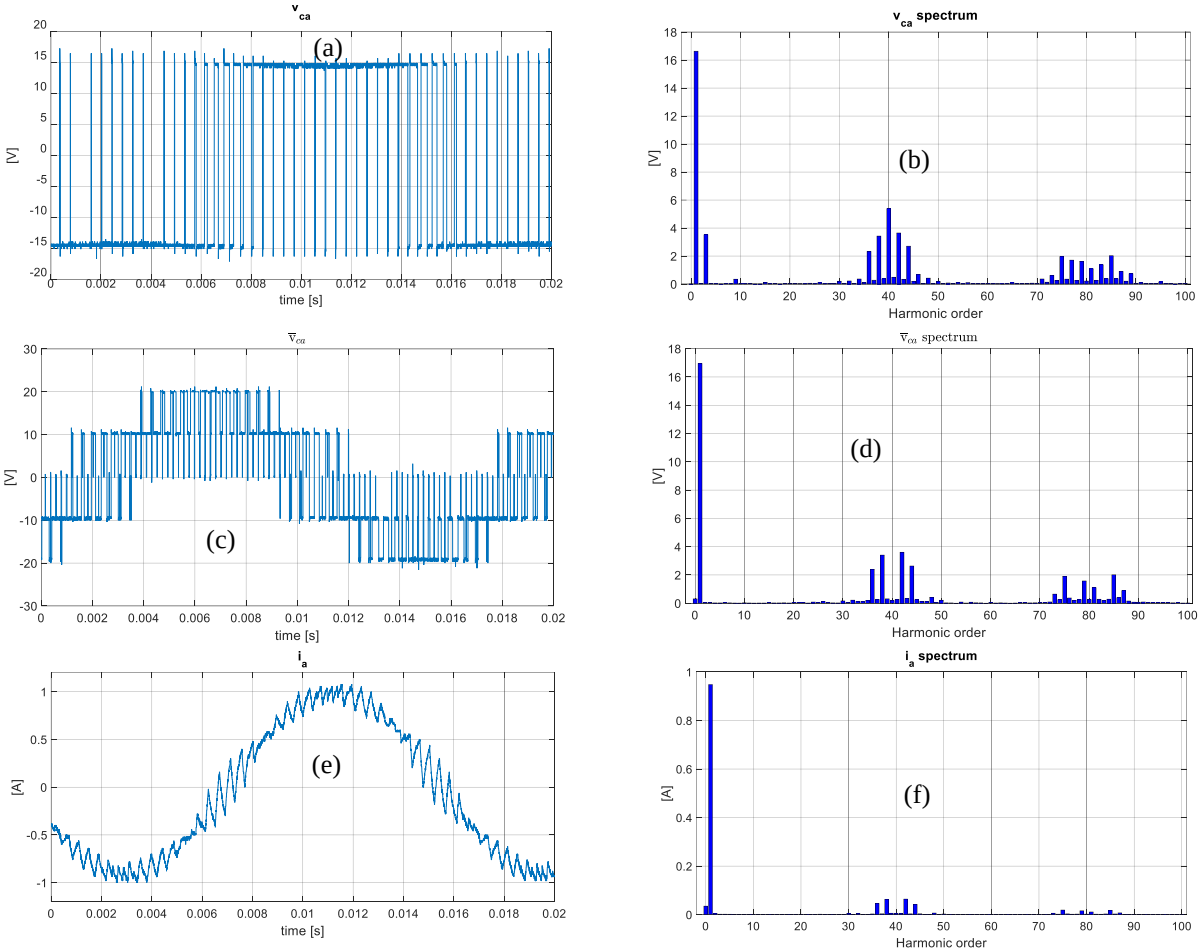


FIGURE 11. a) v_{ca} waveform; b) v_{ca} spectrum; c) $\bar{v}_{ca}=v_a$ waveform; d) $\bar{v}_{ca}=v_a$ spectrum; e) i_a waveform; and f) i_a spectrum. Using m = 115%. (all experimental results)

H. *BASIC CONTROL LOOPS FOR GRID CONNECTED CONVERTERS (3T+2L (1(S+E+T) + 1S))*

To contextualize this set of five classes to the students, they are focused on the problem of connecting a solar panel and its DC/DC boost converter to the grid via a DC/AC converter. Here, the panel together with the DC/DC converter and its Maximum Power Point Tracking (MPPT) control are considered as a current source, that injects the generated power into the DC bus of the DC/AC converter. Almost all the laboratory activities are simulations, but will include additional experimental activities in the near future. Cascaded controllers are learned one by one, from the lowest hierarchy level to the higher. Only grid following strategies are discussed.

In the first theory class, dedicated to the single-phase case, students:

- Learn that many renewable energy generation and storage systems deliver DC voltage, that must be connected to the grid, requiring a DC/AC converter and related control;
- Starting with a synchronous single-phase machine with internal voltage $v_c(t)$ and internal inductance L, connected to the AC grid $v(t)$, calculate $v_c(t)$ required to inject a given $i(t)$ into the grid. The injection of active and reactive currents is revised;
- Verify that the synchronous generator simplified model is equal to the small-signal model of the H-bridge connected to a DC voltage source and to the AC grid via its inductor, with its associated PWM block. So, by imposing as the PWM reference signal $v_{ref}(t)$, the $v_c(t)$ calculated in the previous item, it is possible to theoretically impose any grid current $i(t)$;
- Notice that the method for calculating $v_c(t)$ uses phasors, which require the phasor value of the grid voltage, which in turn requires at least half a cycle to be calculated. Once the new $v_{ref}(t)$ is imposed, the current will take approximately 5L/R seconds to reach steady state, where R is the grid plus the filter resistance. This shows that this $v_{ref}(t)$ calculation strategy is not suitable for real-time operation. Students learn that an internal current loop can solve this problem, by real time calculating the voltage $v_{ref}(t)$ that forces $i(t)$ to track $i_{ref}(t)$ with minimum error.
- Learn that a phase locked loop (PLL) can generate the signals $v_{//}(t)$ and $v_{\perp}(t)$, with unit amplitude, respectively in phase and in quadrature (-90°) with the fundamental component of $v(t)$. So, a sinusoidal reference current containing active and reactive current with amplitudes I_p and I_q respectively is calculated by:

$$i_{ref}(t)=I_p\, v_{//}(t)+I_q\, v_{\perp}(t) \qquad (2)$$

- Learn that for imposing desired values or active power P and reactive power Q, I_p and I_q can be calculated by:

$$I_p=2P/V \qquad I_q=2Q/V \tag{3}$$

where V is the peak value of a sinusoidal $v(t)$.

- Learn that when a renewable with its MPPT is connected to the DC bus of the DC/AC converter, the DC source is substituted by a capacitor. In this case it is impossible to impose P because the renewable source is now generating P_{dc} and if $P \neq P_{dc}$, the capacitor voltage will vary. So, the DC voltage must be regulated by an additional cascaded DC voltage loop, that calculates DC/AC converter P such that $P=P_{dc}$.

In the first laboratory class students:

- Validate, by simulation, step-by-step, the topics in the explanation given at the first theory class;
- Do the experimental validation of the current loop. After obtaining the converter transfer function, Students obtain the tracking and disturbance transfer functions for the single-phase DC/AC converter, using a continuous time domain PI controller, with a simple tunning strategy [33]. The necessity of higher gains to minimize the effect of the disturbance (grid voltage), the strong limitations of the PI controller and the necessity of improved controllers, the role of grid voltage compensation through a feed-forward loop, the anti-windup and the controller discretization are discussed, based on [34], [35]. The lecture experiment uses a 2-level H-bridge converter (Fig. 6) with DC voltage ($V_{DC} = 25V$). inductive filter (L = 14 mH), resistive load (R = 17.2 Ω) on the AC side, switching frequency (f_s = 6 kHz), current tracking loop using a digital PI controller with anti-windup and feedforward of the load voltage for disturbance mitigation. Fig. 12 shows the experimental (12a) and simulated (12b) results, consisting of a reference step response for the resistive load connected to the converter.

The second theory class presents an introduction to Space Vectors [31], to be used in the third theory class.

In the third theory class, the 3-phase case will be controlled in abc and dq coordinates. The control strategy for both is similar to the one proposed for the single-phase case. Students:

- Obtain the state space model of the 3-phase converter and show that it presents strong coupling between the three grid currents and their respective PWM reference voltages. They verify that it is impossible to impose three arbitrary currents because in a 3-phase / 3-wire system the sum of the currents is null;
- Learn a first proposal for current tracking in abc coordinates by using three independent current loops. Simulations are used to show that any attempt to track reference currents whose instantaneous sum is null, but transducers having a small amount of gain or offset error can lead to misoperation and even instability. Since three controllers cannot be employed, the conflict between controllers can be solved according to [36] by using only two currents lops, for phases a and b, producing the PWM reference signals v_{ca_ref} and v_{cb_ref}; The third reference is obtained by $v_{cc_ref}=-(v_{ca_{ref}}+v_{cb_{ref}})$;
- Learn that the phase and quadrature current references for phases a and b, with amplitude I_P and I_q respectively are easily obtained from the in phase and quadrature signals generated by the 3-phase PLL. They have unit amplitude and are in phase and quadrature with the positive sequence of the fundamental grid voltages;
- Obtain I_P and I_q as a function of P and Q respectively;
- Learn that the control can be done in dq coordinates, with only two current controllers, whose references are $i_{ref_d}=I_p$ and $i_{ref_q}=I_q$. Verify that the converter state space model is coupled, but can be easily decoupled by internal feedback [35]. The calculation of I_P and I_q as a function of P and Q is identical to the abc case. The DC voltage loop is identical to the one used for the abc coordinates.

In the second laboratory class, students validate the control of 3-phase case by simulation. In previous lessons, PSIM schematics were provided. In this lesson, students will be required to incorporate the control loops into a provided diagram, which contains only the 3-phase converter and its PWM. They will also be required to propose and implement the minimum tests necessary to validate the operation of the controllers.

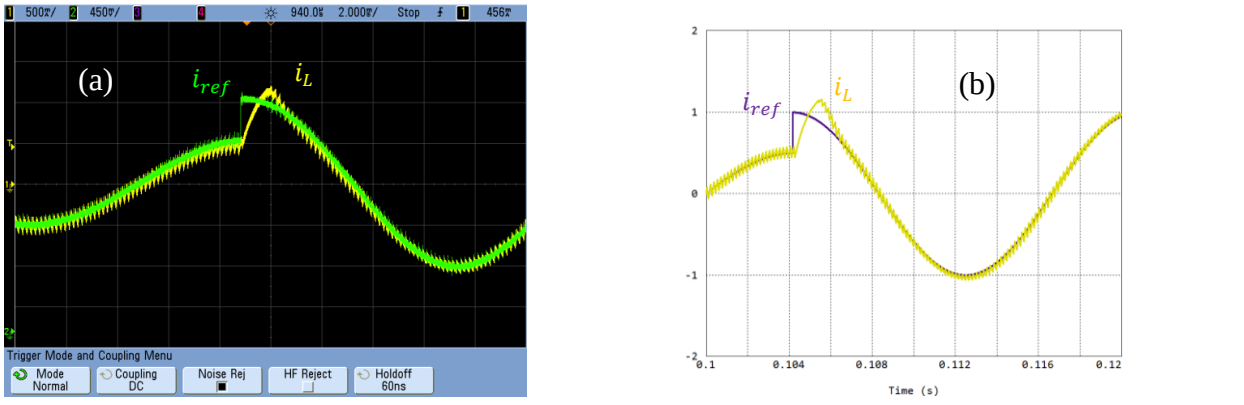


FIGURE 12. Step and tracking response: a) Measured reference current (green - i_{ref}) and load current (yellow - i_L); and b) Simulated reference current (magenta - i_{ref}) and load current (yellow - i_L).

I. *BIDIRECTIONAL DC-DC NON ISOLATED CONVERTER (1T+1L(E+S))*

The HB is used as a bidirectional DC/DC converter according to Fig. 13, that shows some possibilities of load at its right side.

In the first Theory class, students:

- Obtain the relationship between voltages and currents and draw, by hand, the converter waveforms;
- Calculate the mean value of v_o, and verify that it is lower o equal to V_{DC};
- Calculate the mean and peak to peak values of the inductor current as a function of the duty cycle d;
- Calculate input mean current and the input and output power and show that the DC/DC converter behaves like a "DC/DC transformer" with "turns ratio" equal to d.
- Verify that this converter can operate bidirectionally.

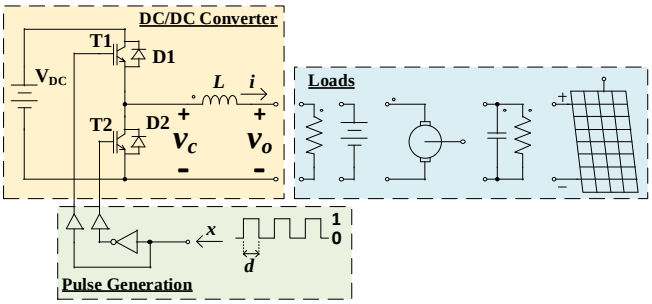


FIGURE 13. Bidirectional DC/DC converter based on half-bridge.

In the laboratory class, the low voltage side is a resistive load ($R=16.6\Omega$), with an LC filter ($L=3.5mH$, $C=2x4,7\mu F$. The high voltage side is a DC power source operating with $V_{DC}=30V$.

Here, students:

- Measure $v_c(t)$, $v_o(t)$ and $i(t)$, their average and peak to peak values validating their corresponding theoretical values;
- Verify that the current ripple is nearly independent of the load resistance, and inductor current becomes negative for low load currents;
- Verify that the mean output voltage is nearly independent of the load current;
- Verify the bidirectional operation by simulation using a battery instead of R and C , as shown in Fig. 13. The experimental validation of this item requires a bidirectional voltage source at V_{DC}, or a setup including diodes and a bleeding resistor. This second option will be implemented in the coming years.
- Verify that in the open loop operation, the current has a slow exponential behavior, that can be overcome with a current loop;
- Discuss applications and verify that it is a two-quadrant converter. They learn that four-quadrant operation can be achieved by using an H-Bridge converter.

J. *OPEN LOOP OPERATION OF BUCK CONVERTER (1T+1L(E+S))*

In the theory class, students are assigned the following tasks:

- Analyze the operation of the bidirectional converter (Fig. 13) when energy flows from V_{DC} to v_o, and concludes that the diode D1 and the transistor T2 never conduct, resulting in the one directional Buck Converter of Fig. 14a [37], [38], simply by extracting these two components from Fig. 13;
- Although they have already analyzed the step-down operation of the bidirectional converter using the well-known half-bridge relationships, they will perform the analysis again, following the method traditionally presented in power electronics textbooks [37], [38]. The authors consider it is important to be able to analyze a circuit in multiple ways. Furthermore, operation in current discontinuity mode does not occur in the bidirectional converter, but it can be adequately analyzed using the classical methodology;
- Understand converter operation, obtain the relationship between currents and voltages for the switch in the ON and OFF conditions, draw the main waveforms and calculate the mean and peak to peak values for the voltages and currents, calculate the power at input and output, and finally students propose a design recipe based on the obtained equations;
- Analyze the waveforms for discontinuous current mode and explain why average output mean voltage increases for lower currents, without calculating it. Discuss the problems caused by this voltage increase and proposes solutions such as bleeding resistor, or voltage controller [38].

In the laboratory class, in order to use the available half-bridge, a Buck Converter is implemented by inserting one Schottky diode as shown in Fig. 14b. Of course, this introduces an additional voltage drop, and its junction capacitance causes excessive voltage ringing, but it is justified by having only one platform to implement DC/AC and DC/DC converters. The ringing is adequately reduced by inserting a RC snubber in parallel with the diode.

For the experiments and simulation: $V_{DC}=30V$, switching frequency f_s=4 kHz, L=3.5mH, C=9.4 μF, duty cycle of 50%, R=20 Ω (continuous conduction mode) and R= 100 Ω (discontinuous conduction mode).

In the laboratory, students:

- Validate theory by simulation and experiments. Fig. 15 shows inductor current i and the voltages v_{oi} and v_o for continuous (Fig. 15a) and discontinuous (Fig. 15b) modes;
- Remove the snubber and see the excessive ringing. The lecturer explains about the junction capacitance and asks them to search for its value in the diode datasheet, and to include the capacitor in the simulation, showing that the ringing frequency, overvoltage and decaying time are consistent with the experimental values.

K. *OPEN LOOP OPERATION OF BOOST CONVERTER (1T+1L(S))*

In the theory class students:

- Verify from the bidirectional converter (Fig. 13) operating with energy flowing from v_o to V_{DC}, that the diode D2 and the transistor T1 are never used. Extracting them from Fig. 13 results in the well-known boost converter [37], [38], not shown here;
- Understand the converter operation, obtain the relationships between voltages and currents,
- Draw the main waveforms, obtain the equations for calculating the current and voltages mean and peak to peak values and propose a recipe for designing the boost converter.

CC BY

Currently, the laboratory class includes only simulation because:

- As explained in the bidirectional DC/DC converter Section, the DC voltage source currently available at the laboratory is not bidirectional;
- The DC/AC converter used in the converter board is the L6203, a 48V, 5A H-Bridge. The power supply input of the chip internal electronics is the same that feeds the DC/AC converter, however, for the boost converter it will be the load voltage. Additional care must be taken in future experiments, to assure that this voltage will never be lower than 12V, to avoid malfunction of gate drivers and internal protection circuits, which is interesting to mention as an implementation aspect during lectures.

In addition to validating the theory results by simulation, students:

- Evaluate the influence of the inductor losses in the converter gain;
- Simulate the converter for discontinuous inductor current, and validate existing equations [38];
- Learn about some important applications of the boost converter and simulate them. They are:
  - Boost interleaved converter: parallel association of boost converter for higher power converters, employing the principle of displaced PWM carriers to reduce ripple at the converter currents and voltages;
  - High power factor rectifier: the popular diode bridge plus boost converter strategy is analyzed along with its cascaded controller, which is similar to the controllers learned for single-phase and 3-phase grid-connected converters;
  - Boost Converter as interface with the DC/AC converter and MPPT for solar panels: based on the VxI and PxI curves of a solar panel, implements a Perturb & Observe MPPT strategy.

L. *OTHER DC/DC CONVERTERS (1T)*

The last theory class is a conventional lecture which briefly presents:

- The non isolated Buck-Boost converter [37], [38];
- The isolated Forward, Flyback converters [37], [38];
- The bidirectional isolated Dual Active Bridge [39] and its one directional version, the Single Active Bridge [38];
- The converters for wireless power transfer [40];
- The analysis of schematics of commercial power supplies and EV chargers.

M. *ACTIVE FILTER (1L(S))*

A simple single-phase active filter, consisting of an H-Bridge, a current loop based on a PI controller and the harmonics calculation based on a simple notch filter to calculate the fundamental component i_1 of the load current i_{load}. The current loop reference current is i_{ref}=-(i_{load}-i_1). The load is a capacitive filter rectifier.

In this laboratory students:

- Simulate the active filter and measure the harmonics attenuation, verifying the improvement of the THD of the line current;
- Reduce the converter DC voltage and are asked to explain why the filter performance worsened. The lecturer explains that the lower DC voltage reduces the converter performance to track currents with high slopes (high frequency, high amplitude harmonics). One solution is to increase the DC voltage, that requires higher voltage rated switches and capacitor. Other solution is to reduce the value of the inductive filter, at the expense of increasing the current high frequency ripple. Also, higher switching frequency will be necessary to synthesize wide band current signals.

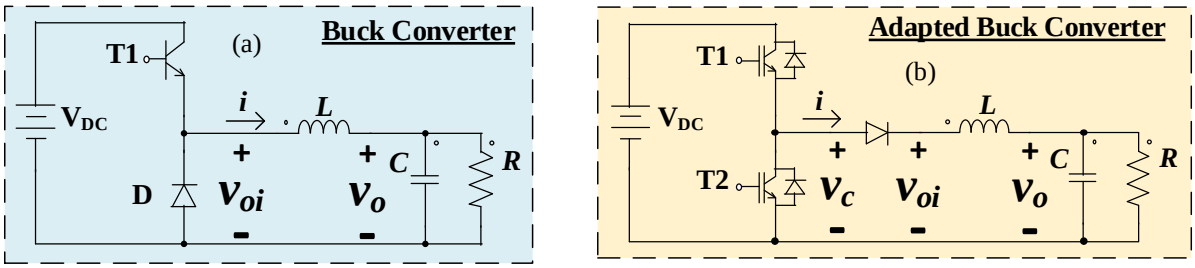
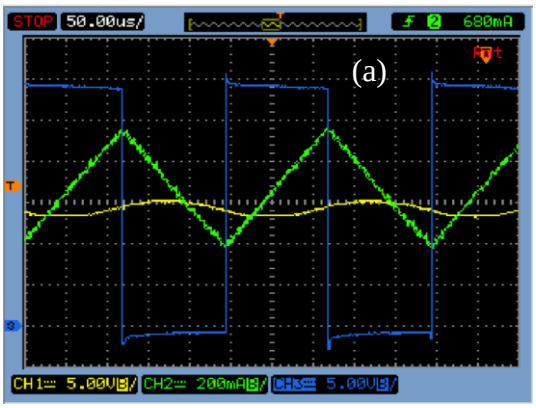


FIGURE 14. a) Buck converter; b) adapted bidirectional converter to operate as a Buck.



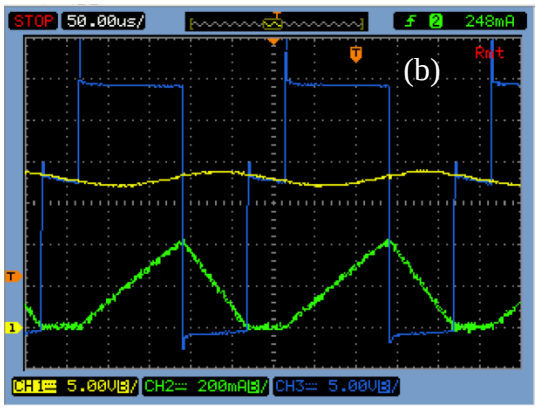


FIGURE 15. v_{oi} (blue); i (green) and v_o (yellow) for: a) continuous and b) discontinuous modes (experimental results).

V. STUDENTS PERFORMANCE ASSESMENT

Despite the importance of student assessment in the teaching-learning process, the heavy workload over the past three years—involving the implementation of experiments and their corresponding scripts, the creation of written materials and theoretical activities, and the updating and revision of all content—compelled us to adopt a simpler yet varied assessment approach, one intended for refinement in the coming years. This approach comprises a grade for the in-class theoretical activity (an individual grade for work performed collectively, called "ME"), a grade for individual experimental reports (a group grade, called "ML"), and a grade for two conventional written exams (individual grades, called "MP"). The evolution of the mean grades is shown in Table 1 and shows a steady increase in the student performance between 2022-2025;

TABLE 1. Response distribution parameters for methodology rating.

Dataset	n	ML	ME	MP
2022	22	7.9	8.4	5.1
2023	19	9.3	9.5	5.3
2024	28	9.4	6.9	6.0
2025	33	8.7	9.2	6.5

VI. DISCUSSION ON THE RESULTS OF METHODOLOGY EVALUATION BY THE STUDENTS

After the beginning of the restructuring, in 2022, among the 28 students that contributed to the study, when asked if the methodology is adequate [20] 46,4% pointed that is it adequate and improvements are necessary.

This is a relevant figure; therefore, the lecturers decided to answer this request and have then continued the improvement of the methodology as described in the paper.

In [41], several modern methodologies, including problem-based learning, case-based learning, flipped classroom, team-based learning, and lecture-based learning are compared in a meta-analysis, evidencing the diversity of methods available in education and showing methods for statistical comparison.

To assess the results of the application of the proposed methodology over the last years, statistical and language model-based analyses methods are used. The goal is not to execute extensive tests on a large set of different methodologies.

A. *STATISTICAL ANALYSIS*

To analyze evidence generated by scores of student evaluation forms and compare different teaching methodologies [41], the analysis of variance (ANOVA) method has been successfully applied in engineering [42], [43] courses.

In this method, when analyzing different samples with different means and variances, it is possible to test and verify the hypothesis that the difference between the means of the samples is significant or not [42].

The analysis has been conducted in 3 sample sets, corresponding to the offerings of Self-Commutated Power Electronics course in the years of 2023, 2024 and 2025. Amongst other questions, students were asked to assess how the offering has satisfied their learning objectives and if the course organization and methodology has been adequate. The possible ratings ranged between 0 (zero), meaning total disagreement, and 5 (five), meaning total agreement.

The distributions of the answers obtained are shown in Figure 6.

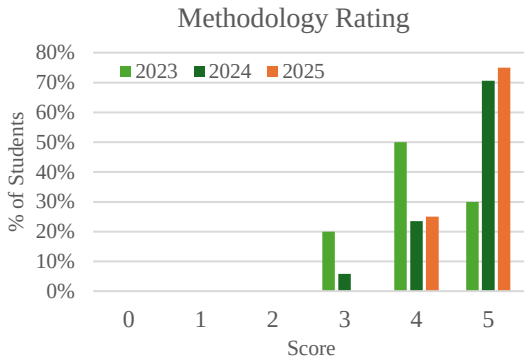


FIGURE 16. Results of the statistical analysis for methodology rating.

It is important to note that there is a significant challenge when engaging students to spontaneously answer the forms, considering that there are approximately 16 students in each of the three classes all offerings.

Next, in Table 2 the response results are presented. The ANOVA [44] results in a $p < 0.05$, meaning there is less than a 5% probability that the differences in the group means are caused by chance (thus rejecting the null hypothesis that all dataset means are equal).

TABLE 2. Response distribution parameters for methodology rating.

Dataset	n	Mean	Standard Deviation
2023	10	4.1000	0.7379
2024	17	4.4671	0.6063
2025	4	4.7500	0.5000

Comparing the distributions in Figure 16, it is possible to see that between the offerings of 2023 and 2024, there has been an increase of 40% in the number of the responses of the students that are totally satisfied with the methodology.

Looking at the results of the offerings, there is also a decrease in the variance throughout the years, showing an increase in the coherence of the responses.

The authors have also added a question in asking students to evaluate if their learning objectives have been met. The results obtained are shown in Figure 17 and Table 3.

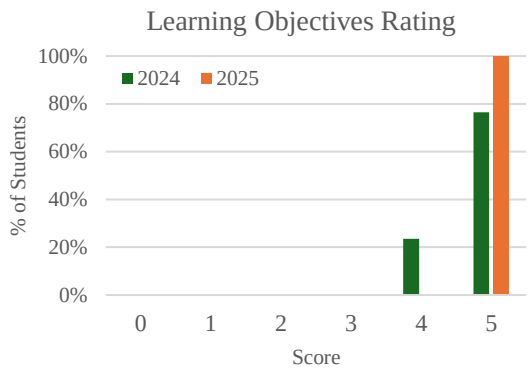


FIGURE 17. Results of the statistical analysis.

TABLE 3. Response distribution parameters for learning objectives rating.

Dataset	n	Mean	Standard Deviation
2024	17	4.7647	0.4372
2025	4	5.0000	0.0000

Even though this is an incomplete comparison, it shows that students agree that their learning objectives are being met. In the last years, the standardized forms used in the department have been applied. In a future work a specific one, better suited for methodology evaluation will be used.

B. *SENTIMENT ANALYSIS*

In the field of education, Large Language Models (LLMs) have been reported as a useful tool for sentiment analysis in student feedback [45]. In this application, textual data containing anonymized textual data obtained from evaluation forms is processed by the model to identify feedback that reveals a positive, neutral or negative sentiment toward the course. A comparative study of several state-of-the-art models in such task has shown that Google Gemini has better accuracy than ChatGPT, Bing, Claude and LlaMa [46], therefore it is chosen by the authors for this analysis.

The methodology used consists in the following steps: i) collecting student feedback, ii) extracting textual data, iii) querying model for sentiment analysis, iv) summarizing the results.

The obtained results are reviewed by the lecturers and reveal a positive view of the didactic value and pedagogical engagement. Students highlight the continuous integration between theoretical content and experimental practice, which facilitates the consolidation of theoretical concepts by allowing direct observation of the real operation and applications of the circuits.

Additionally, the appreciation of the platform made available is evidenced, as well as the recognition of the commitment, the knowledge and the receptive posture of the lecturers throughout the monitoring of the experiments.

The main point of friction lies in the established schedules, with frequent delays in the practical sessions (three sequential classes to accommodate 16 students each class).

Additionally, it is pointed out that the excessive extension of theory test scripts and lab reports, added to the fast pace of classes and the high density of students per experimental bench (reaching up to four students per group), reduces the practical dynamics, compromising deep conceptual reflection.

Given the feedback received, the authors suggest in the future allowing enough time for the classes and execution of the assigned tasks, adjusting to the rhythm of the students. This will be achieved by reducing the number of items in the theory and lab activities. Also, it is important to have a reduced number of students per group, to reduce oversharing of the resources available.

VII. CONCLUSIONS AND FUTURE WORK

This paper discusses the restructuring of power electronics lectures using an active learning methodology, focusing on the strong correlation between theory, simulations and experiments. The motivation is to overcome the limitations of the previous course based on conventional methodologies. The restructuring allowed: i) an increase in the amount of content covered, ii) an increase in the abilities acquired by students, compared to the former strategy with separate theory (30 x 100 minutes classes/semester) and laboratory (15 x 100 minutes classes/semester) courses, iii) to keep students aligned with the topics being studied; iv) to prepare students to benefit from experimental lectures, by engaging with modeling, analysis, and experimental/simulation validation, rather than merely follow procedures; v) to show students that modeling errors increase when simplifying assumptions fail and motivate model improvements; vi) the improvement in grade performance from year to year ; and vii) the increase of students satisfaction.

Items i-v) are based on the perception of the lecturers, while item vi) is measured by the grades obtained by the students in the various diversified activities. Finally, item vii) is measured through statistical analysis and LLM-based sentiment analysis and show a steady increase in the student satisfaction with the methodology and the outcomes related to their learning objectives. Preliminary course assessment indicates an increase of 40% in the number of the responses of the students that are totally satisfied with the methodology, while students praised the integration of theory and experimental classes, which contributed to their learning objectives.

Regarding the course content, it has become useful to include topics on power quality throughout the program, given the growing number of power electronics applications in the electrical grid. The likelihood of a student having to design power electronics equipment is low compared to the opportunities to work on the grid integration of such equipment and on solving power quality issues.

It is important to highlight that the experimental platform cited in this paper [7], [8], as well as a new platform for line commutated converters [47] under development, is available as open-source hardware and software [19]. In the future works, authors are working to improve the student performance evaluation strategies together with the whole course assessment.

ACKNOWLEDGMENTS

The authors thank all graduate and undergraduate students that have contributed in the development of the experimental platform during the last decade.

This study was financed in part by the several grants received, including CNPq, FAPESP 2016/16542-5, Coordenação de Aperfeiçoamento de Pessoal de Nível Superior – Brasil (CAPES) – Finance Code 001 and by Amigos da Poli Endowment Fund.

AUTHOR'S CONTRIBUTIONS

L.MATAKAS JUNIOR: Conceptualization, Data Curation, Formal Analysis, Funding Acquisition, Investigation, Methodology, Project Administration, Resources, Software, Supervision, Validation, Visualization, Writing – Original Draft, Writing – Review & Editing. **V.N.MACHADO:** Conceptualization, Data Curation, Formal Analysis, Investigation, Methodology, Resources, Software, Supervision, Validation, Visualization, Writing – Review & Editing. **W.KOMATSU:** Conceptualization, Formal Analysis, Funding Acquisition, Investigation, Methodology, Project Administration, Resources, Supervision, Validation, Visualization, Writing – Review & Editing. **L.KOLEFF:** Conceptualization, Formal Analysis, Funding Acquisition, Investigation, Methodology, Project Administration, Resources, Software, Supervision, Validation, Visualization, Writing – Review & Editing.

PLAGIARISM POLICY

This article was submitted to the similarity system provided by Crossref and powered by iThenticate – Similarity Check.

DATA AVAILABILITY

The data used in this research is available in the body of the document.

REFERENCES

[1] N. Mohan and S. Raju, *Power electronics, a first course: simulations and laboratory implementations*, Second edition. Hoboken, New Jersey: John Wiley & Sons, 2023. URL: https://www.wiley.com/en-us/power-electronics-a-first-course-simulations-and-laboratory-implementations-2nd-edition-p-9781119818588.

[2] U. Drofenik and J. W. Kolar, "Survey of modern approaches of education in power electronics," in *APEC. Seventeenth Annual IEEE Applied Power Electronics Conference and Exposition (Cat. No.02CH37335)*, Dallas, TX, USA: IEEE, 2002, pp. 749–755. doi: 10.1109/APEC.2002.989329.

[3] L. P. D. Silva *et al.*, "Low-cost didactic module for single-phase inverter teaching," in *2017 Brazilian Power Electronics Conference (COBEP)*, Juiz de Fora: IEEE, Nov. 2017, pp. 1–6. doi: 10.1109/COBEP.2017.8257232.

[4] J. A. Pomilio, "Atividades Didáticas Experimentais em Eletrônica de Potência: Convergindo Conhecimentos e Tecnologias," *Eletrônica Potência*, vol. 25, no. 2, pp. 146–153, Jun. 2020, doi: 10.18618/REP.2020.2.0023.

[5] J. V. G. França *et al.*, "Development of a Didactic Platform for Flexible Power Electronic Converters," *Eletrônica Potência*, vol. 27, no. 3, pp. 225–235, Aug. 2022, doi: 10.18618/REP.2022.3.0012.

[6] A. Al Bastami, A.-T. Avestruz, and S. B. Leeb, "Teaching modeling, control, and simulation in a modular kit for power electronics," in *2014 IEEE 15th Workshop on Control and Modeling for Power Electronics (COMPEL)*, Santander, Spain: IEEE, Jun. 2014, pp. 1–10. doi: 10.1109/COMPEL.2014.6877151.

[7] L. Koleff *et al.*, "Development of a Modular Open Source Power Electronics Didactic Platform," in *2019 IEEE 15th Brazilian Power Electronics Conference and 5th IEEE Southern Power Electronics Conference (COBEP/SPEC)*, Santos, Brazil: IEEE, Dec. 2019, pp. 1–6. doi: 10.1109/COBEP/SPEC44138.2019.9065327.

[8] L. Koleff *et al.*, "Open Source Modular Didactic Platform for Power Electronics Teaching," in *Engenharia Elétrica e de Computação: Atividades Relacionadas com o Setor Científico e Tecnológico 2*, 1st ed., Atena Editora, 2020, pp. 179–203.

[9] D. H. C. Santos, B. de A. Coutinho, A. S. Cordeiro, M. M. Stopa, and A. F. Cupertino, "A Case Study of a Didactic Platform Experiments using Off-the-Shelf Hardware," *Eletrônica Potência*, vol. 30, pp. e202501–e202501, Jan. 2025, doi: 10.18618/REP.e202501.

[10] P. F. Donoso-Garcia, P. C. Cortizo, and L. M. F. Morais, "Ensino Orientado Ao Projeto: Uma Experiência Para O Ensino De Eletrônica Nas Disciplinas De Laboratório De Eletrônica E Eletrônica De Potência," *Eletrônica Potência*, vol. 13, no. 2, pp. 109–116, May 2008, doi: 10.18618/REP.2008.2.109116.

[11] D. Dujic, A. Cervone, C. Li, P. Bontemps, and Y. Frei, "Teaching Power Electronics: How to Achieve the Desired Learning Outcomes?," *IEEE Power Electron. Mag.*, vol. 9, no. 4, pp. 45–53, Dec. 2022, doi: 10.1109/MPEL.2022.3216094.

[12] T. Caldognetto, A. Petucco, A. Lauri, and P. Mattavelli, "A flexible power electronic converter system with rapid control prototyping for research and teaching," *HardwareX*, vol. 14, p. e00411, Jun. 2023, doi: 10.1016/j.ohx.2023.e00411.

[13] Z. Zhang, C. T. Hansen, and M. A. E. Andersen, "Teaching Power Electronics With a Design-Oriented, Project-Based Learning Method at the Technical University of Denmark," *IEEE Trans. Educ.*, vol. 59, no. 1, pp. 32–38, Feb. 2016, doi: 10.1109/TE.2015.2426674.

[14] F. S. Garcia, A. A. Ferreira, and J. A. Pomilio, "Plataforma De Ensino De Eletrônica De Potência Versátil E De Baixo Custo," *Eletrônica Potência*, vol. 13, no. 2, pp. 85–90, May 2008, doi: 10.18618/REP.2008.2.085090.

[15] E. A. Vendrusculo, A. A. Ferreira, and J. A. Pomilio, "Plataforma Didática Para Avaliação Rápida E Experimental De Estratégias De Controle Em Eletrônica De Potência," *Eletrônica Potência*, vol. 13, no. 2, pp. 99–108, May 2008, doi: 10.18618/REP.2008.2.099108.

[16] N. Mohan *et al.*, "Restructuring of first courses in power electronics and electric drives that integrates digital control," *IEEE Trans. Power Electron.*, vol. 18, no. 1, pp. 429–437, Jan. 2003, doi: 10.1109/TPEL.2002.807120.

[17] "European Low Voltage Directive 2014/35/EU." [Online]. URL: https://eur-lex.europa.eu/legal-content/EN/TXT/HTML/?uri=CELEX:32014L0035.

[18] "NR-10 Brazilian Safety Regulatory Standard." [Online]. URL: https://www.gov.br/trabalho-e-emprego/pt-br/acesso-a-informacao/participacao-social/conselhos-e-orgaos-colegiados/comissao-tripartite-partitaria-permanente/normas-regulamentadora/normas-regulamentadoras-vigentes/norma-regulamentadora-no-10-nr-10.

[19] "LEP – Laboratório de Eletrônica de Potência – Power Electronics Laboratory | Departamento de Engenharia de Energia e Automação Elétricas | Departamento de Engenharia de Energia e Automação Elétricas." Accessed: Sep. 08, 2025. [Online]. URL: https://www.pea.usp.br/Lep.

[20] V. N. Machado, F. O. Martinz, W. Komatsu, and L. Matakas Junior, "Laboratory Supported Lectures on Modeling: Transformer Case," *Eletrônica Potência*, vol. 29, p. e202427, Aug. 2024, doi: 10.18618/REP.2005.1.006011.

[21] V. N. Machado, F. O. Martinz, W. Komatsu, and L. M. Junior, "Proposed Set of Power Quality Lectures for an Undergraduate Power Electronics Course," in *2023 IEEE 8th Southern Power Electronics Conference and 17th Brazilian Power Electronics Conference (SPEC/COBEP)*, Florianopolis, Brazil: IEEE, Nov. 2023, pp. 1–8. doi: 10.1109/SPEC56436.2023.10407483.

[22] L. M. Junior, V. N. Machado, and W. Komatsu, "Proposal of an Experimentally Aided Methodology for Learning Self-Commutated DC/AC and DC/DC Converters in Undergraduate Classes," in *2025 Brazilian Power Electronics Conference (COBEP)*, Oct. 2025, pp. 1–6. doi: 10.1109/COBEP66423.2025.11231619.

[23] V. B. Bhavaraju and P. N. Enjeti, "Analysis and design of an active power filter for balancing unbalanced loads," *IEEE Trans. Power Electron.*, vol. 8, no. 4, pp. 640–647, Oct. 1993, doi: 10.1109/63.261037.

[24] W. Kaiser, W. Komatsu, and W. Pó, "Harmonic instability in channel induction furnaces induced by static converters," presented at the European Conference on Power Electronics and Applications, Firenze, 1991, pp. 247–251.

[25] R. W. Erickson and D. Maksimović, *Fundamentals of power electronics*, Third edition. Cham: Springer, 2020, doi: 10.1007/978-3-030-43881-4.

[26] E. W. Kimbark, *Direct current transmission*. New York: Wiley-Interscience, 1971. ISBN: 978-0-471-47580-4.

[27] D. G. Holmes and T. A. Lipo, *Pulse width modulation for power converters: principles and practice*. in IEEE series on power

engineering. Hoboken, NJ: John Wiley, 2003, doi: 10.1109/9780470546284.

[28] H. Black, Modulation Theory. New York: D. Van Nostrand Company, 1953.

[29] H. Akagi, "Classification, terminology, and application of the modular multilevel cascade converter (MMCC)," in *The 2010 International Power Electronics Conference - ECCE ASIA -*, Sapporo, Japan: IEEE, Jun. 2010, pp. 508–515. doi: 10.1109/IPEC.2010.5543243.

[30] W. Komatsu and L. Matakas Junior, "A Didactic Comparison Of Space-Vector PWM And Carrier-Based PWM With Optimal Zero-Sequence Injection," presented at the 8º Congresso Brasileiro de Eletrônica de Potência (COBEP), 2005, pp. 175–181.

[31] L. Matakas Junior, "Controller implementation for three phase power converters without coordinate transformations: geometric analysis based on space vectors," Departamento de Engenharia de Energia e Automação Elétricas, USP, 2012. URL: https://teses.usp.br/teses/disponiveis/livredocencia/3/tde-18052012-163756/publico/LivreDocenciaLourencoMatakasJr2012.pdf.

[32] T. L. Grant and T. H. Barton, "Control Strategies for PWM Drives," *IEEE Trans. Ind. Appl.*, vol. IA-16, no. 2, pp. 211–216, Mar. 1980, doi: 10.1109/TIA.1980.4503773.

[33] F. O. Martinz, R. D. Miranda, W. Komatsu, and L. Matakas, "Gain limits for current loop controllers of single and three-phase PWM converters," in *The 2010 International Power Electronics Conference - ECCE ASIA -*, Sapporo, Japan: IEEE, Jun. 2010, pp. 201–208. doi: 10.1109/IPEC.2010.5543860.

[34] F. O. Martinz, "Study of AC current control techniques in VSC-PWM converters in ABC stationary coordinate system," Thesis, Universidade de São Paulo, 2013.

[35] S. Buso and P. Mattavelli, *Digital Control in Power Electronics*. 2006, doi: 10.2200/S00047ED1V01Y200609PEL002.

[36] D. G. Holmes, T. A. Lipo, B. P. McGrath, and W. Y. Kong, "Optimized Design of Stationary Frame Three Phase AC Current Regulators," *IEEE Trans. Power Electron.*, vol. 24, no. 11, pp. 2417–2426, Nov. 2009, doi: 10.1109/TPEL.2009.2029548.

[37] N. Mohan, T. M. Undeland, and W. P. Robbins, *Power electronics: converters, applications, and design*, 2. ed. New York, NY: Wiley, 1995. ISBN: 978-0-471-58408-7.

[38] D. W. Hart, *Power electronics*. in Connect, learn, succeed. New York, NY: McGraw-Hill, 2011. URL: https://www.mheducation.com/highered/product/power-electronics-hart.

[39] R. Baranwal, G. F. Castelino, K. Iyer, K. Basu, and N. Mohan, "A Dual-Active-Bridge-Based Single-Phase AC to DC Power Electronic Transformer With Advanced Features," *IEEE Trans. Power Electron.*, vol. 33, no. 1, pp. 313–331, Jan. 2018, doi: 10.1109/TPEL.2017.2669148.

[40] A. H. Moret and L. Matakas, "Analysis of the possibilities for control-free voltage and current source operation of 'wireless power transfer - wpt' systems," in *2015 IEEE 13th Brazilian Power Electronics Conference and 1st Southern Power Electronics Conference (COBEP/SPEC)*, Fortaleza: IEEE, Nov. 2015, pp. 1–6. doi: 10.1109/COBEP.2015.7420196.

[41] X. Li *et al.*, "Comparison of the effects of different teaching methods on the effectiveness of teaching neurology in China: a bayesian network meta-analysis and systematic review," *BMC Med. Educ.*, vol. 24, no. 1, p. 1560, Dec. 2024, doi: 10.1186/s12909-024-06397-9.

[42] C. P. de Carvalho, M. B. Silva, B. N. Aihara, and E. P. Ferreira, "Comparison of Different Types of Active Learning in a Course of Industrial Engineering," in *Proceedings of 15th Intenational CDIO Conference*, Arhus, Denmark: Aarhus University, 2023, pp. 212–220. doi: 10.7146/aul.347.

[43] S. Sreemahadevan and V. G, "A case study on the comparison of teaching–learning and performance evaluation methods applied to engineering students," *Educ. Inf. Technol.*, vol. 29, no. 13, pp. 17621–17633, Sep. 2024, doi: 10.1007/s10639-024-12559-5.

[44] W. F. Guthrie, "NIST/SEMATECH e-Handbook of Statistical Methods (NIST Handbook 151)." National Institute of Standards and Technology, 2020. doi: 10.18434/M32189.

[45] J. Hwang, "LLMs for Sentiment Analysis in Education: A Study in Resource-Limited Settings," thesis, Purdue University Graduate School, 2025. doi: 10.25394/PGS.28543865.v1.

[46] B. S. Ortiz Quispe, A. M. Tafur Gomez, and E. A. Alfaro Paredes, "Comparative study of chatbots for sentiment analysis," *Humanit. Soc. Sci. Commun.*, Jul. 2026, doi: 10.1057/s41599-025-06411-5.

[47] L. Koleff, L. Araújo, M. Zambon, W. Komatsu, E. Pellini, and L. M. Junior, "A Flexible Didactic Platform for Thyristor-Based Circuit Topologies," *Eletrônica Potência*, vol. 25, no. 2, pp. 154–162, Jun. 2020, doi: 10.18618/REP.2020.2.0012.

BIOGRAPHIES

Lourenco Matakas Junior received the B.S., M.S., and Ph.D. degrees in electrical engineering from the Polytechnic School of the University of São Paulo (EPUSP), Sao Paulo, in 1984, 1989, and 1998. He is an Associate Professor at EPUSP. His research focuses on topologies, control and application of static converters connected to the grid, phase-locked loops, WPT and Modular Multilevel Converters. He is a member of the Brazilian Power Electronics Society (SOBRAEP), Brazilian Society of Automatics (SBA) and of the Institute of Electrical and Electronics Engineers (IEEE).

Vinícius N. Machado born in 18/07/2001 in São Paulo, Brazil, received the B.S., and M.S. degrees in electrical engineering from the Polytechnic School of the University of São Paulo (EPUSP), São Paulo, in 2023 and 2026. He is currently working towards the Ph.D. degree in electrical engineering from the Federal University of Minas Gerais, Belo Horizonte. His areas of interest are: power electronics, power quality, electronic control systems, microgrids, grid-connected power converters modeling and control, and grid-forming converters. Mr. Machado is a student member of the Brazilian Power Electronics Society (SOBRAEP).

Wilson Komatsu born in São Paulo, Brazil, in 1963. He received the B.S., M.S., and Ph.D. degrees in electrical engineering from the Polytechnic School of the University of São Paulo (EPUSP), São Paulo, in 1986, 1992, and 2000, respectively. He is an Associate Professor of power electronics at EPUSP. His research areas are control and modeling of static converters, and their application to electrical power systems and electrical power quality. Dr. Komatsu is a member of the Institute of Electrical and Electronics Engineers (IEEE) and of the Brazilian Power Electronics Society (SOBRAEP).

Lucas Koleff born in São Paulo, Brazil, in 1991, received his B.Sc. degree with honors from the University of São Paulo, Brazil, his D.D. M.Sc. degree from the Technical University of Darmstadt, Germany in 2015 and his Ph.D. degree from the University of São Paulo, Brazil, in 2021. Between 2021 and 2026 he worked in the industry as an R&D project manager. Since 2026 he has been a Professor of Electrical Engineering at the Polytechnic School of the University of São Paulo. His current research interests are power converters modelling and control, digital twins, grid resilience and novel applications in power systems.